Xu *et al. Geoscience Letters* (2022) 9:25
https://doi.org/10.1186/s40562-022-00234-x

Geoscience Letters

RESEARCH LETTER

Open Access

Robustness of the long-term nonlinear evolution of global sea surface temperature trend

Zhenhao Xu[1,3], Gang Huang[1,2,3*], Fei Ji[4,5*], Bo Liu[6], Fei Chang[7] and Xichen Li[8]

Abstract

The multi-scale variability of global sea surface temperature (GSST), which is often dominated by secular trends, significantly impacts global and regional climate change. Previous studies were mainly carried out under linear assumptions. Even if the nonlinear evolution patterns have been discussed based on annual-mean data, the conclusions are still insufficient due to several factors. Here, based on the Ensemble Empirical Mode Decomposition (EEMD) method, the robustness of GSST trends tied to the sampling frequency and time interval selection is further explored. The main features derived from the annual-mean data are maintained. However, monthly and seasonal-mean data both mute the cooling in the equatorial central Pacific and the Southern Ocean in the Pacific sector, meanwhile intensify and expand the warming over the North Pacific. The results also highlight that early data cause a minimal effect on secular trends except for the portion near the start point of the interval due to the local temporal nature of EEMD. Overall, the long-term GSST trends extracted by EEMD have good robustness. Our research also clarifies that quadratic fitting cannot reveal all the meaningful evolution patterns, even as a nonlinear solution.

Keywords: Global sea surface temperature, Robustness analysis, EEMD, Nonlinear trends

Introduction

It is undeniable that the accumulated greenhouse gases (GHGs) caused by human activities lead to remarkable warming of the climate system, widely covering the atmosphere, hydrosphere, and land surface, which has profoundly affected natural ecosystems and human social activities (IPCC 2021; Huang et al. 2022).

As an essential component of the climate system, the ocean, especially for several critical regions, is highly associated with global and regional climate change (Kosaka and Xie 2013, 2016; Yao et al. 2017). Due to its vast surface, enormous mass, and heat capacity, the ocean essentially regulates the Earth's Energy Imbalance arising from the so-called greenhouse effect (Chen and Tung 2014). It is also confirmed that the ocean absorbs over 90% of the surplus heat from GHGs since the mid-nineteenth century (Levitus et al. 2000, 2012; Trenberth et al. 2014; Nieves et al. 2015; Cheng et al. 2019). What's more, 2021 is the new warmest year for the world ocean despite La Niña conditions, according to reliable ocean heat content (OHC) records by humans (Cheng et al. 2022). Nevertheless, the momentum and heat exchange between the ocean and the atmosphere is substantially related to the sea surface temperature anomaly (SSTA) (Deser et al. 2010). It has also been revealed that multi-scale climate change is dramatically influenced by the variabilities of sea surface temperature (SST), typically dominated by secular trends (Yao et al. 2017; Chen and Tung 2017; Zhang et al. 2019). Thus, a deeper understanding of the long-term evolution of global sea surface temperature

*Correspondence: hg@mail.iap.ac.cn; jif@lzu.edu.cn

[1] State Key Laboratory of Numerical Modeling for Atmospheric Sciences and Geophysical Fluid Dynamics, Institute of Atmospheric Physics, Chinese Academy of Sciences, Beijing 100029, China
[4] College of Atmospheric Sciences, Lanzhou University, Lanzhou 730000, China
Full list of author information is available at the end of the article

(GSST) is beneficial to the understanding of climate change.

As mentioned by Xu et al. (2021), previous studies of long-term trends in GSST were primarily based on linear assumptions, yet there was no evidence indicating that the intrinsic trends are linear (Wu et al. 2007; IPCC 2013). Therefore, previous studies discussed the long-term trend based on an adaptive and nonlinear method named EEMD (Huang et al. 1998; Huang and Wu 2008; Wu and Huang 2009; see more details in Sect. 2) and illuminated the region-dependent warming fact of GSST's centennial trend with a novel perspective. However, there are still a few gaps that previous studies carried out investigations based on annual-mean data to reduce computation costs, while the sampling frequency may change the secular trends by affecting the extraction process of the EEMD method. Another factor is the insufficient quality of early observations, whose impacts on the findings cannot be arbitrarily ignored. Accordingly, although the nonlinear trend has been examined in some detail, there is still a shortage of information as well as an incomplete frame about its robustness of regional evolution features, and further discussion is needed.

Here, to explore the long-term nonlinear evolution trend of GSST more comprehensively, the robustness of the conclusions with different sampling frequencies is discussed by comparison in terms of monthly, seasonal-mean, and annual-mean data, respectively. Furthermore, considering observation resolution was very sparse in the early twentieth century, the first 20 and 40 years of GSST will also be removed, respectively. We also aim to investigate whether a priori quadratic fitting may reveal some meaningful patterns.

The other sections are arranged as follows: Sect. 2 describes the SST dataset and details of the research methodology. In Sect. 3, the robustness of GSST trends tied to the sampling frequency and time interval selection is demonstrated. What's more, this section also shows the intrinsic trends derived from quadratic fitting. Finally, Sect. 4 summarizes and discusses this study.

Data and method

Data

We used the Extended Reconstructed Sea Surface Temperature dataset (version 5) (ERSST v5) from the National Oceanic and Atmospheric Administration (NOAA) with a spatial resolution of $2^\circ \times 2^\circ$, which provides global monthly SST from 1854 to the present (Huang et al. 2017). In this study, the time interval was limited to 1900–2020. We averaged the monthly SST data into seasonal-mean and annual-mean data, respectively.

The EEMD method

In recent years, time–frequency analysis methods have expanded rapidly. Much attention has been paid to the Ensemble Empirical Mode Decomposition (EEMD) method, which is suitable for adaptive and local analysis of the nonlinear and nonstationary time series (Huang and Wu 2008; Wu and Huang 2009). EEMD is an improvement of the Empirical Mode Decomposition (EMD) method (Huang et al. 1998), which effectively overcomes a problem named "Mode mixing", i.e., any IMF consisting of oscillations with quite disparate timescales simultaneously due to the intermittency of the driving mechanisms (Wu and Huang 2009).

A brief procedure of the EEMD decomposition is demonstrated as follows:

(i) Add a group of white noise $\varepsilon_i(t)(i = 1, 2, 3 \ldots N)$ to $SSTA(t)$, respectively:

$$x_i(t) = SSTA(t) + \varepsilon_i(t), \tag{1}$$

where $x_i(t)$ and $\varepsilon_i(t)$ are the ith new white-noise-added series and realization white noise sequence with amplitude equal to a specific ratio of the standard deviation of $x(t)$, respectively. N is the ensemble number. The intensity of the white noise should be a proper value. Signals dominated by low frequency should use smaller amplitude, and vice versa. According to Wu and Huang (2009), the white noise is applied with a standard deviation of 0.2;

(ii) Located all the maxima (minima) of the time series and connected them with a cubic spline interpolation as an upper (lower) envelope for each $x_i(t)$;

(iii) Define the mean of upper and lower envelopes as $m_i(t)$, then compute the difference between $x_i(t)$ and $m_i(t)$ to yield a new series $h_i(t)$:

$$h_i(t) = x_i(t) - m_i(t); \tag{2}$$

(iv) Judge that $h_i(t)$ meets the qualifications for being Intrinsic Mode Function (IMF), denoted as $c_{1i}(t)$. Here, the two conditions are (a) the number of zero-crossings and extrema are equal to or differs by at most one; (b) the averaged sequence of the upper and lower envelopes is zero among the whole period (Huang et al. 1998). $c_{1i}(t) = h_i(t)$ is established if the conditions above are satisfied; otherwise, just set $x_i(t) = h_i(t)$, repeat steps (ii)–(iv) until established. Then extract $c_{1i}(t)$ from the original series:

$$f_i(t) = x_i(t) - c_{1i}(t); \tag{3}$$

(v) Regard $f_i(t)$ as a new original series just like $x_i(t)$ and repeat the above steps (ii)–(iv) to obtain other IMFs, i.e., $c_{2i}(t), c_{3i}(t) \ldots, c_{mi}(t)$, until residual

becomes a strictly monotonic function or with only one extremum, marked as $r_i(t)$;

(vi) Obtain the ensemble means of corresponding IMFs and the secular trend of the decompositions as a result:

$$c_j(t) = \lim_{N\to\infty}\frac{1}{N}\sum_{i=1}^{N} c_{ji}(t)\big(j = 1, 2, 3\ldots, m\big), \tag{4}$$

$$r(t) = \lim_{N\to\infty}\frac{1}{N}\sum_{i=1}^{N} r_i(t). \tag{5}$$

Thus, in EEMD, a time series $x(t)$ at each grid is decomposed into several amplitude–frequency-modulated oscillatory components $c_j(t)$ and $r(t)$, which is a curve either monotonic or containing only one extremum:

$$SSTA(t) = \sum_{j=1}^{m} c_j(t) + r(t). \tag{6}$$

Note that Eq. (6) is an asymptotic relation when the ensemble number approaches infinity. Thus, the larger ensemble number leads to a better approximation. Here, following Xu et al. (2021), the ensemble number (N) is set to 400. Besides, the number of $c_j(t)$ is determined as follows:

$$m = \lfloor \log_2 M \rfloor - 1, \tag{7}$$

where M is the length of a time series. Since the time interval of the study was restricted to 1900–2020, the values of m were 5, 8, and 10, corresponding to annual-mean, seasonal-mean, and monthly data, respectively.

Benefiting from the adaptive and local nature of the EEMD method, the obtained amplitude–frequency-modulated IMFs and secular trend are free from any priori subjective assumptions, utterly data-driven. What's more, the conclusions are almost irrelevant to the time interval selection, which means they do not suffer from the interference of newly introduced data (Wu and Huang 2009; Qian et al. 2010; Wu et al. 2011, 2022; Ji et al. 2014; Wei et al. 2019; Xu et al. 2021).

EEMD trend and warming rate

Here, a grid-by-grid decomposition of SSTA is analyzed by the EEMD method (Wu et al. 2009, 2022; Ji et al. 2014; Xu et al. 2021). Following Ji et al. (2014), we define the EEMD trend of a time series as:

$$Trend(t) = r(t) - r(t_0). \tag{8}$$

Here, t_0 refers to 1900. Since the long-term trend extracted by EEMD is a continuous function, the EEMD trend of June and summer (averaged from June to August) will be selected and presented to represent the specific year, respectively, for monthly and seasonal-mean data. We also clarify that similar results can be reached when other months or seasons are employed.

In addition, the instantaneous warming rate is then defined as the derivative of EEMD trend, numerically approximated by calculating the central difference quotient. For example, the instantaneous warming rate in 1950 for yearly data should be written as $Rate(1950) = (Trend(1951) - Trend(1949))/2$. When focusing on seasonal-mean and monthly data, the right-hand side of the equation above will be replaced with $4 * \big(Trend(1950_{Autumn}) - Trend\big(1950_{Spring}\big)\big)/2$ and $12 * \big(Trend\big(1950_{July}\big) - Trend\big(1950_{May}\big)\big)/2$, respectively.

Results

Long-term evolution of GSST trends tied to the sampling frequency

Each ocean basin has several principal patterns, such as El Niño-Southern Oscillation (ENSO), Pacific Decadal Oscillation (PDO), and Atlantic Multidecadal Oscillation (AMO), etc., ranging from interannual to multi-decadal timescales. Yet, the secular trend dominates the largest variance contribution, corresponding to the well-known "global warming". Here, after EEMD decomposition, the internal variability modes of the SST series are removed into IMFs, and what is extracted are the long-term trends defined previously. Although Xu et al. (2021) characterized the nonlinear evolution of GSST from an annual-mean perspective under the consideration of reducing computational cost, the sampling frequency of the data may affect the decomposition process and thus the magnitude even direction of secular trend. In this section, the discrepancy of the results derived from monthly, seasonal-mean, and annual-mean SST, respectively, will be compared with the aim of enhancing the comprehensive understanding of the robustness of previous findings.

As shown in Fig. 1, the main features of the long-term nonlinear evolution trends are identical, but still have visually discernable differences. Before 1910, only the EEMD trends derived from annual-mean data show cumulative changes that could be noticed (> 0.3 K or < − 0.3 K), as reflected in the weak cooling of the equatorial central Pacific. By 1925, the EEMD trend derived from monthly and seasonal-mean data appears to have slight cooling in the equatorial central Pacific, while the magnitude and extent are much smaller than in annual-mean data. Meanwhile, the warmer regions are relatively more similar among different periods, while the warming signal over the North Pacific is intensified. Another distinctive feature is that the annual-mean data show a cooling pattern in the Southern Ocean in the Pacific sector, while the remaining groups appear near the 1940s.

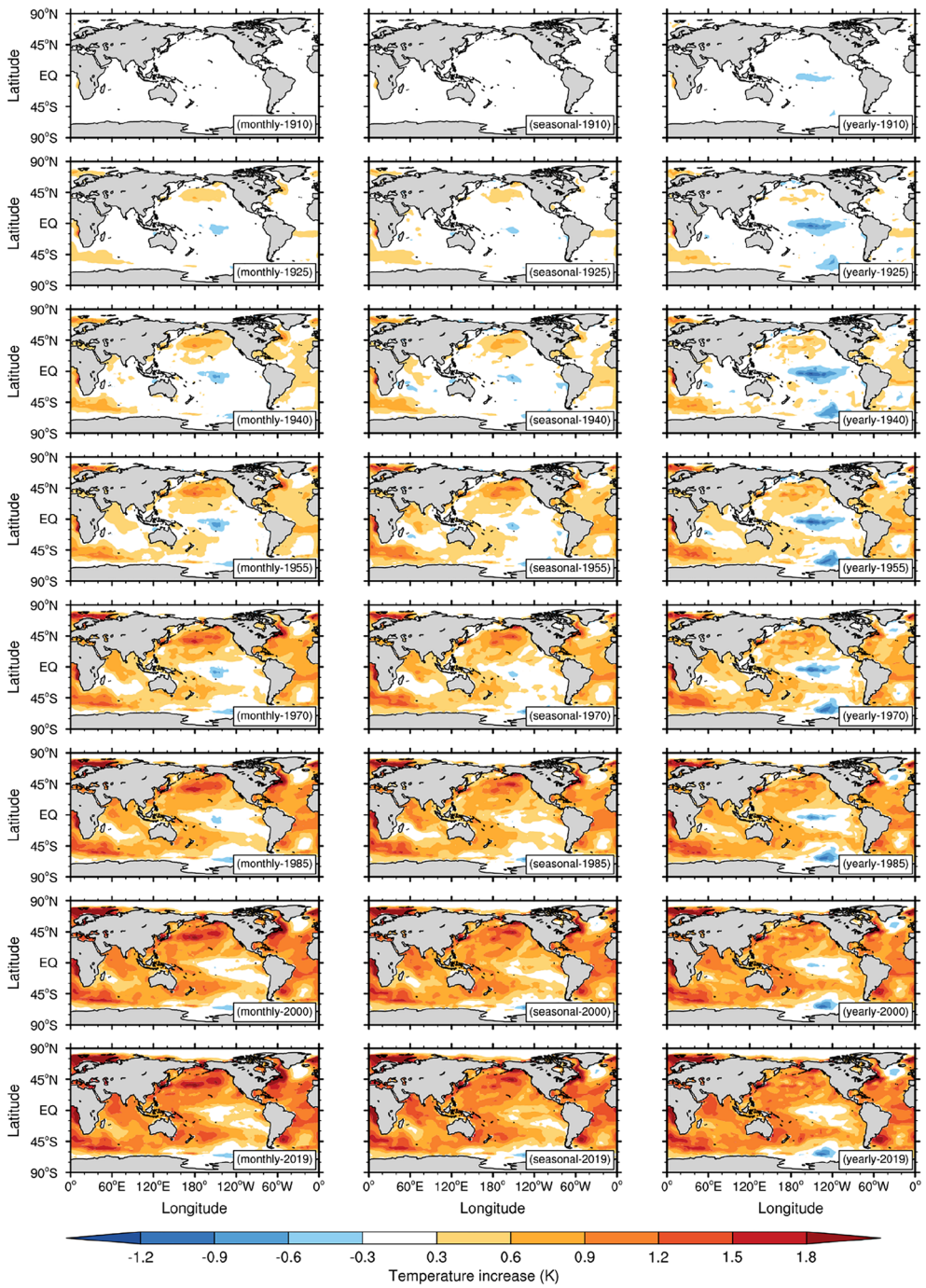

Fig. 1 Spatial evolution of the EEMD trend of global sea surface temperature tied to the sampling frequency. From top to bottom, the EEMD trend ended in 1910, 1925, 1940, 1955, 1970, 1985, 2000, and 2019, respectively. From left to right, EEMD trends are derived from monthly, seasonal, and annual data, respectively. Note that the color bar is the same as Xu et al. (2021) and below

Around the mid-twentieth century, the negative pattern in the equatorial central Pacific began to shrink. Correspondingly, there was also a dramatic reversal of the instantaneous warming rate in this region, with cooling marked contraction and a shift to rapid warming (see Additional file 1: Fig. S1). From the mid-twentieth century to the early twenty-first century, the magnitude of EEMD trends has been increasing in most regions

(acceleration of warming rate, shown in Additional file 1: Fig. S1), whereas the North Atlantic Ocean conversely experienced a continuous cooling.

For the EEMD trend from 1900 to 2019, the equatorial central Pacific still shows no visually detectable warming, except for seasonal-mean data. Also, the Southern Ocean in the Pacific sector has a negative EEMD trend related to the circulation dynamics of the Southern Ocean (Speer et al. 2000; Long et al. 2020; Xu et al. 2022). On the other hand, the North Atlantic has a so-called "warm hole" (Drijfhout et al. 2012; Woollings et al. 2012; Marshall et al. 2015), although it is relatively weak in the EEMD trend derived from monthly data. The heaviest warming occurs over several regions, including the Arctic Ocean, the entire Indian Ocean, east of the continents in the northern hemisphere, the Southern Ocean from the tip of South Africa expanded to the Indian Ocean, the Gulf of Guinea, and the eastern tropical Atlantic Ocean is pretty consistent.

In summary, the cooling trends over the equatorial central Pacific and the Southern Ocean in the Pacific sector retrieved from the monthly and seasonal-mean datasets are relatively weaker compared to that of the annual-mean datasets, meanwhile intensify and expand the warming trends over the North Pacific. Apart from that, the primary features are comparatively consistent, indicating better robustness of the conclusion regarding sampling frequency. Noticeably, the sampling frequency has almost no effect on the findings obtained from previous linear assumptions since no extraction process of IMFs is involved (see Additional file 1: Figs. S2 and S3).

Warming rate of GSST trends tied to the time interval selection

Climatological studies on GSST have been suffering from a dilemma in both record length and accuracy of observation data. In the early twentieth century, ship-based archives were extremely coarse and sparse, risking distortion of the SST field obtained by several statistical approaches. In contrast, despite the high spatial resolution of satellite data in recent years, the short observation period does not apply to some studies on longer time scales, such as climate variability on multi-decadal scales or long-term trends.

Here, to explore how the nonlinear secular trends extracted by the EEMD method are affected by the earlier data, the SST data during the period 1900–1920 and 1900–1940 are removed, respectively. We arbitrarily select two points located in the South Atlantic and the equatorial Pacific, obtaining their annual-mean series for preliminary analysis, with the results shown in Fig. 2. For comparison and visual presentation, the anomaly series are all relative to the 1900–2020 baseline period for either choice of the time interval.

The EEMD decomposition process necessitates connecting all the extrema to yield the envelope, which is vital in extracting IMFs. While only the maximum/minimum value can be determined by the information at the endpoints of the interval, the other side is available in a non-completely objective way. As a result, spurious oscillations can occur near the endpoints, known as the "end effect". In Fig. 2a, the long-term trend of a regional mean SST in the South Atlantic, especially in the early period, shows some differences when the time interval investigated is changed. The other one, located in the equatorial east-central Pacific, inspires a more dramatic phenomenon (see Fig. 2b). The first cooling and then warming feature around the 1940s revealed by Xu et al. (2021) is replaced by persistent rapid warming when the first 20 years or more of the data are removed.

The warming rate is better than the EEMD trend here to compare the details of these cases because the latter highly relies on the secular trend in 1900, which is unavailable when the early data are absent. Thus, Fig. 3 shows the warming rate of GSST related to the time interval selection.

Around 1925, the extensive and intense cooling rate in the equatorial central Pacific and the southern part of the Southern Ocean in the Pacific sector was replaced by mild warming trend in case the first two decades were removed. It seems that the Southern Ocean, in general, appears to have a larger magnitude of warming rate. In addition, the cooling pattern in the North Atlantic, the Arctic Ocean, and the Southern Indian Ocean is largely enhanced, replacing the original warming features, by the 1940s, the Southern Ocean in the Pacific sector completely converted to a warming pattern. After the mid-twentieth century, the SST of the first two decades slightly affects the evolution rate, consistent with the case shown in Fig. 2. While at this time, the noticeable warming/cooling area precipitous dropped but the warming was enhanced over the Southern Ocean directly opposite Australia and the South Atlantic, the cooling over the North Atlantic, for the absence of the first 40 years of SST. Sporadic cooling signals were also reported across the Pacific and Indian Oceans. During recent decades, especially in 2019, the most rapid warming occurred in the Arctic Ocean, the entire Indian Ocean, the western boundary current and their extensions in both hemispheres, and the tropical central Pacific Ocean, respectively, no matter of any case. Yet the more extended period of SST removal, the more significant magnitude of the warming rate and the keener cooling in the region of the Southern Ocean adjacent to the Antarctic.

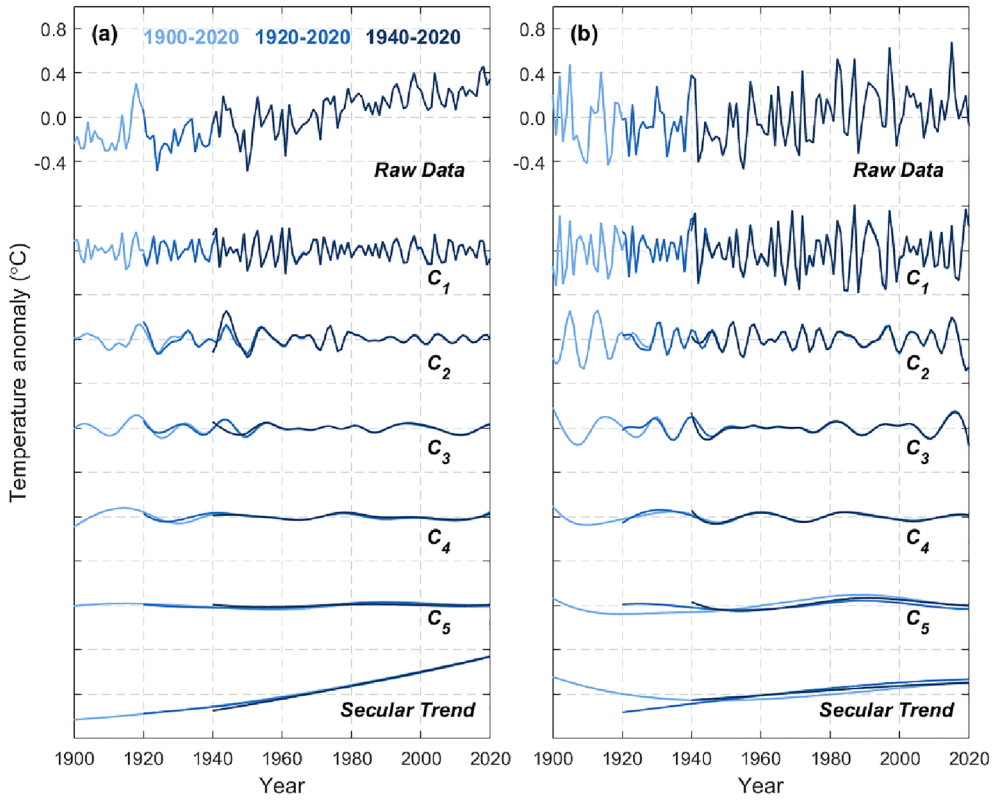

Fig. 2 The temporal locality of EEMD decomposition of the annual SSTA at **a** (42°S—46°S, 58°W—54°W) averaged in the South Atlantic; **b** (2°S—2°N, 122°W—118°W) averaged in the equatorial Pacific. From top to bottom, the curves represent the raw data, EEMD components (c_j), and secular trend. The curves are colored from light to dark in each panel, representing 1900–2020, 1920–2020, and 1940–2020, respectively

The intrinsic trends derived from quadratic fitting

One of the most striking features of the GSST nonlinear evolution over the past century is that the equatorial eastern Pacific and the Southern Ocean in the Pacific sector first experienced a cooling followed by a warming in the middle of the last century (Xu et al. 2021), which implies that the EEMD trend is not monotonic in these regions. While the property of EEMD dictates that the long-term trend has at most one extreme in the whole span (Wu et al. 2007), it is natural to consider whether the quadratic function, although logically a priori, could expose some similar characteristics?

Similar to the EEMD trend, the internal trend derived from quadratic fitting is defined as $Trend_{qua}(t) = curve_{qua}(t) - curve_{qua}(t_0)$, which is present in Fig. 4. Compared with the left column of Fig. 1, in terms of early cooling, the tropical Central Pacific is invisible ($\left|Trend_{qua}(t)\right| < 0.3K$), the Southern Ocean narrowed dramatically, and only the Southwest Indian Ocean had a weak expansion. By 2019, the intrinsic trend shows warming almost everywhere except the North Atlantic, while the equatorial central Pacific and the Southern Ocean exhibit noticeable warming. The strongest warming also occurs over the Arctic Ocean, the Indian Ocean, east of the continents, the Southern Ocean to the east of South Africa, the Gulf of Guinea, and the eastern tropical Atlantic Ocean. On the whole, the spatial distribution obtained from the quadratic fitting appears flatter and smoother than the EEMD trend, which presumably embodies a more significant spatial coherence.

Although the intrinsic trends derived from quadratic fitting retain several evolutionary features, many significant phenomena have been obscured. The conclusions above indicate that a priori quadratic fitting may not reveal all the meaningful patterns as EEMD, even if it is also a nonlinear solution.

Conclusions and discussion

As the greenhouse effect induces the accumulation of heat surpluses in the climate system, the response of SST to global warming is not homogeneous but shows a clear regional feature. Although the long-term evolution of the GSST trend was displayed by annual-mean data from 1900, the EEMD decomposition involves a multi-step extraction, which may be affected by several factors such

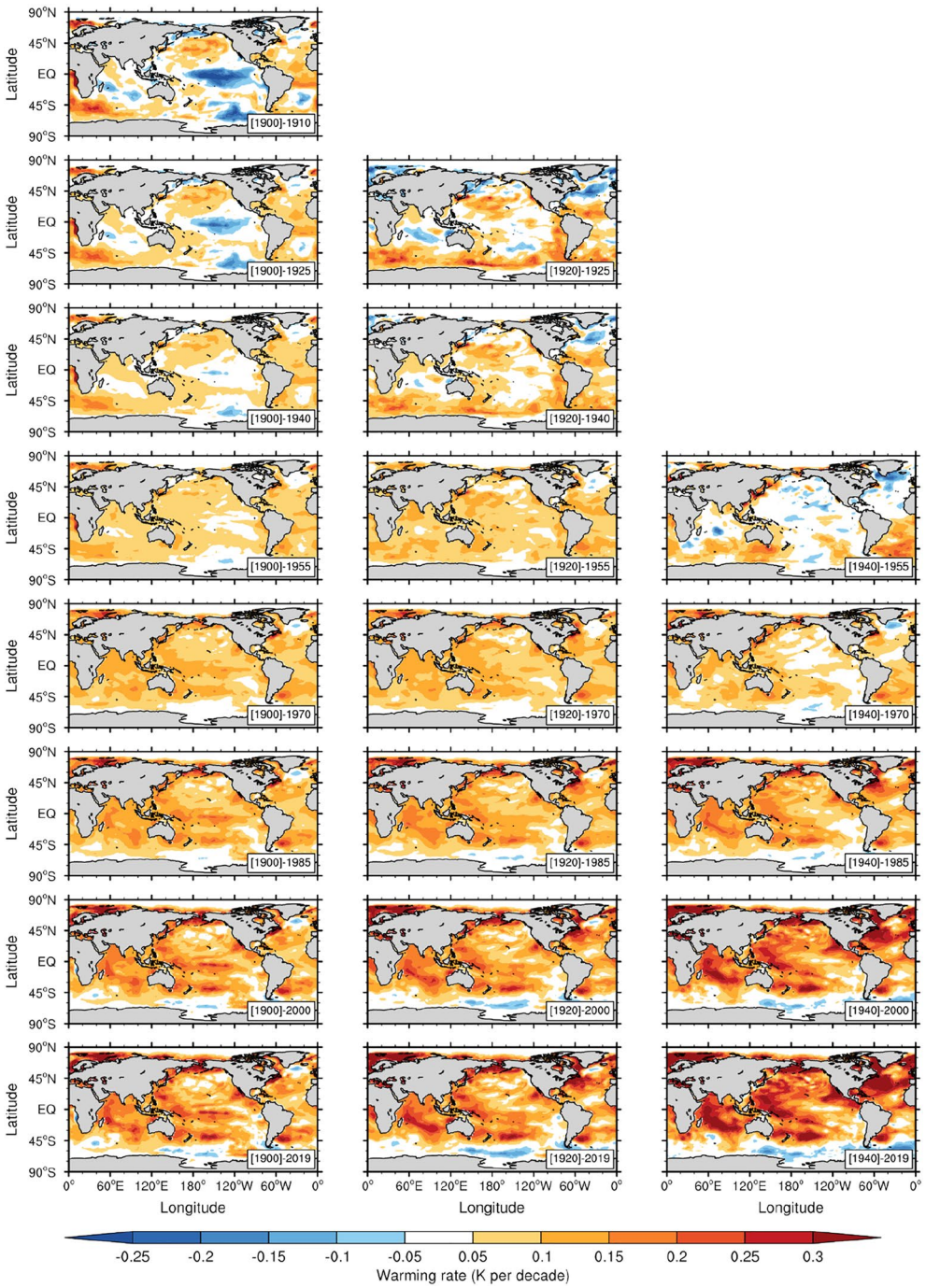

Fig. 3 Warming rate of global sea surface temperature tied to the time interval selection. From top to bottom, the instantaneous warming rate of the secular trend in 1910, 1925, 1940, 1955, 1970, 1985, 2000, and 2019, respectively. From left to right, the instantaneous warming rates are all derived from the annual data, but the time interval is 1900–2020, 1920–2020, and 1940–2020, respectively

as the sampling frequency and the time interval. This study further discusses the robustness of the nonlinear evolution trend, despite some numerical differences, as a hint for future research.

By contrasting the EEMD trend in different cases, we found that the primary features derived from monthly/seasonal-mean data are pretty consistent with annual-mean data. However, they also mute the cooling in the

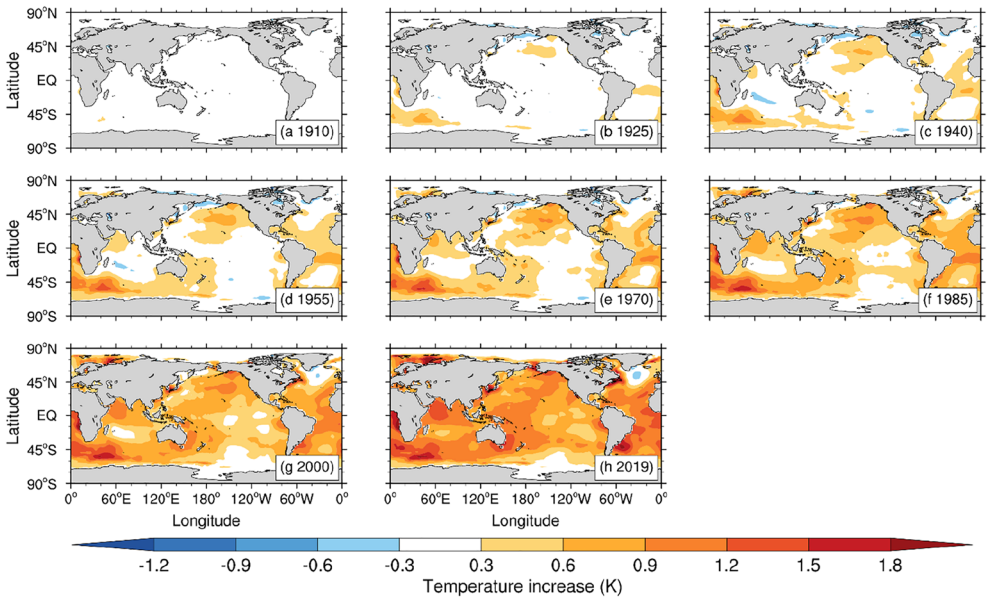

Fig. 4 Spatial evolution of the intrinsic trends of global sea surface temperature derived from a quadratic fitting. (a–h) The intrinsic trends ending in 1910, 1925, 1940, 1955, 1970, 1985, 2000, and 2019, respectively

equatorial central Pacific and the Southern Ocean in the Pacific sector while emphasizing more warming over most North Pacific in both magnitude and surface area. It is still unclear whether extra-tropical physical processes drive the phenomena revealed by these statistical tools, and the related mechanisms need to be further investigated. Besides, the last part of our study also specifies that the quadratic fitting scheme does not successfully reveal the long-term evolution trends. Actually, there is no a priori way to know which areas are intrinsically characterized by such trend features, which is also logically incompatible.

As for the time interval of the EEMD decomposition, the secular trends usually suffers from the uncertainties of the reconstructed datasets, especially when the early record due to the World Wars were primarily based on the sparse ship-based observation. Taking advantage of the temporal localization of EEMD, variation is only induced near the left endpoint of the interval when the early data are removed, as long as the number of IMFs is invariant, according to formula (8). It is also important to point out that, for all three cases covered in that section, the secular trends obtained by the longer SST may mask potential oscillations stuck between their whole span, making the final evolution trends different.

In conclusion, exploring the nonlinear evolution of GSST trends contributes to a comprehensive understanding of the climate system's response to global warming. This research aims to enrich and refine the conclusions from the nonlinear perspective disclosed by the EEMD decomposition, which provides new evidence for the robustness of several findings. Even though the physical mechanisms are not fully explained, we believe our work lays a stronger research foundation for future efforts.

Supplementary Information

The online version contains supplementary material available at https://doi.org/10.1186/s40562-022-00234-x.

Additional file 1: Figure S1. Warming rate of global sea surface temperature tied to the sampling frequency. **Figure S2.** The spatial structure of temperature increase based on time-unvarying linear trend over the whole data domain from 1900 to 2019. **Figure S3.** Warming rate of global sea surface temperature derived from a quadratic fitting. **a**–**h** the instantaneous warming rate of the intrinsic trends in 1910, 1925, 1940, 1955, 1970, 1985, 2000, and 2019, respectively.

Acknowledgements
This work was supported by the National Natural Science Foundation of China (42141019, 41831175, 91937302, 41721004, 41875083, and 42075029), Key Deployment Project of Centre for Ocean Mega-Research of Science, Chinese academy of science (COMS2019Q03), and Strategic Priority Research Program of Chinese Academy of Sciences (XDA20060501). We also would like to thank Prof. Jing Li for her helpful suggestions.

Author contributions
ZX, GH, and FJ conceived the study. ZX wrote the initial manuscript in discussion with GH, ZX and BL contributed to the data analysis and produced figures. XL and FJ improved the manuscript. All authors contributed to interpreting results, discussion, and revision of this paper. All authors read and approved the final manuscript.

Data availability
NOAA_ERSST_V5 data provided by the NOAA/OAR/ESRL PSD, Boulder, Colorado, USA, from their website at https://www.esrl.noaa.gov/psd/.

Declarations

Competing interests
The authors declare no conflicts of interest in this work.

Author details
[1]State Key Laboratory of Numerical Modeling for Atmospheric Sciences and Geophysical Fluid Dynamics, Institute of Atmospheric Physics, Chinese Academy of Sciences, Beijing 100029, China. [2]Laboratory for Regional Oceanography and Numerical Modeling, Qingdao National Laboratory for Marine Science and Technology, Qingdao 266237, China. [3]University of Chinese Academy of Sciences, Beijing 100049, China. [4]College of Atmospheric Sciences, Lanzhou University, Lanzhou 730000, China. [5]Collaborative Innovation Center for Western Ecological Safety, Lanzhou University, Lanzhou 730000, China. [6]School of Information Science and Engineering, Lanzhou University, Lanzhou 730000, China. [7]Gansu Air Traffic Management Sub-Bureau of Civil Aviation Administration of China, Lanzhou 730000, China. [8]International Center for Climate and Environment Sciences, Institute of Atmospheric Physics, Chinese Academy of Sciences, Beijing 100029, China.

Received: 2 March 2022 Accepted: 27 June 2022
Published online: 09 July 2022

References

Chen X, Tung KK (2014) Climate. Varying planetary heat sink led to global-warming slowdown and acceleration. Science 345:897–903
Chen X, Tung K-K (2017) Global-mean surface temperature variability: Space–time perspective from rotated eofs. Clim Dyn 51:1719–1732
Cheng L, Abraham J, Hausfather Z, Trenberth KE (2019) How fast are the oceans warming? Science 363:128–129
Cheng L, Abraham J, Trenberth KE, Fasullo J, Boyer T, Mann ME, Zhu J, Wang F, Locarnini R, Li Y et al (2022) Another record: Ocean warming continues through 2021 despite La Nina conditions. Adv Atmos Sci 39:373–385
Deser C, Alexander MA, Xie SP, Phillips AS (2010) Sea surface temperature variability: Patterns and mechanisms. Ann Rev Mar Sci 2:115–143
Drijfhout S, van Oldenborgh GJ, Cimatoribus A (2012) Is a Decline of AMOC causing the warming hole above the North Atlantic in observed and modeled warming patterns? J Clim 25(24):8373–8379
Huang NE, Wu Z (2008) A review on Hilbert-Huang transform: Method and its applications to geophysical studies. Rev Geophys. https://doi.org/10.1029/2007RG000228
Huang NE, Shen Z, Long SR, Wu MC, Shih HH, Zheng Q, Yen N-C, Tung CC, Liu HH (1998) The empirical mode decomposition and the Hilbert spectrum for nonlinear and non-stationary time series analysis. Proc R Soc Lond A Math Phys Sci 454:903–995
Huang B, Thorne PW, Banzon VF, Boyer T, Chepurin G, Lawrimore JH, Menne MJ, Smith TM, Vose RS, Zhang H (2017) Extended reconstructed sea surface temperature, version 5 (ERSSTv5): upgrades validations, and intercomparisons. J Clim 30(20):8179–8205
Huang G, Xu Z, Qu X, Cao J, Long S, Yang K, Hou H, Wang Y, Ma X (2022) Critical climate issues towards carbon neutrality targets. Fundam Res 2(2022):396–400. https://doi.org/10.1016/j.fmre.2022.02.011
Ji F, Wu Z, Huang J, Chassignet EP (2014) Evolution of land surface air temperature trend. Nat Clim Chang 4:462–466
Kosaka Y, Xie SP (2013) Recent global-warming hiatus tied to equatorial pacific surface cooling. Nature 501:403–407
Kosaka Y, Xie S-P (2016) The tropical pacific as a key pacemaker of the variable rates of global warming. Nat Geosci 9:669–673
Levitus S, Antonov JI, Boyer TP, Stephens C (2000) Warming of the world ocean. Science 287:2225–2229
Levitus S, Antonov JI, Boyer TP, Baranova OK, Garcia HE, Locarnini RA, Mishonov AV, Reagan JR, Seidov D, Yarosh ES et al (2012) World ocean heat content and thermosteric sea level change (0–2000 m) 1955–2010. Geophys Res Lett. https://doi.org/10.1029/2012GL051106
Long S, Liu Q, Zheng X et al (2020) Research progress of long-term ocean temperature changes in the southern ocean. Adv Earth Sci 35(9):962–977. https://doi.org/10.11867/j.issn.1001-8166.2020.076
Marshall J et al (2015) The oceans role in the transient response of climate to abrupt greenhouse gas forcing. Clim Dyn 44:2287–2299
Nieves V, Willis JK, Patzert WC (2015) Global warming. Recent hiatus caused by decadal shift in indo-pacific heating. Science 349:532–535
Qian C, Wu Z, Fu C, Zhou T (2010) On multi-timescale variability of temperature in china in modulated annual cycle reference frame. Adv Atmos Sci 27:1169–1182
Speer K, Rintoul SR, Sloyan B (2000) The diabatic Deacon cell. J Phys Oceanogr 30(12):3212–3222
Trenberth KE, Fasullo JT, Balmaseda MA (2014) Earth's Energy Imbalance. J Clim 27(9):3129–3144
Wei M, Qiao F, Guo Y, Deng J, Song Z, Shu Q, Yang X (2019) Quantifying the importance of interannual, interdecadal and multi-decadal climate natural variabilities in the modulation of global warming rates. Clim Dyn 53:6715–6727
Woollings T, Gregory JM, Pinto JG, Reyers M, Brayshaw DJ (2012) Response of the North Atlantic storm track to climate change shaped by ocean-atmosphere coupling. Nat Geosci 5:313–317
Wu Z, Huang NE (2009) Ensemble empirical mode decomposition: A noise-assisted data analysis method. Adv Adapt Data Anal 01:1–41
Wu Z, Huang NE, Long SR, Peng CK (2007) On the trend, detrending, and variability of nonlinear and nonstationary time series. Proc Natl Acad Sci U S A 104:14889–14894
Wu Z, Huang NE, Chen X (2009) The multi-dimensional ensemble empirical mode decomposition method. Adv Adapt Data Anal 01:339–372
Wu Z, Huang NE, Wallace JM et al (2011) On the time-varying trend in global-mean surface temperature. Clim Dyn 37(3–4):759–773
Wu W, Ji F, Hu S, He Y, Wei Y, Xu Z, Yu H (2022) Future evolution of global land surface air temperature trend based on Coupled Model Intercomparison Project Phase 6 models. Int J Climatol. https://doi.org/10.1002/joc.7668
Xu Z, Ji F, Liu B, Feng T, Gao Y, He Y, Chang F (2021) Long-term evolution of global sea surface temperature trend. Int J Climatol 41:4494–4508
Xu X, Liu J, Huang G (2022) Understanding Sea Surface Temperature Cooling in the central-east Pacific sector of the Southern Ocean during 1982–2020. Geophys Res Lett. https://doi.org/10.1029/2021GL097579
Yao S-L, Luo J-J, Huang G, Wang P (2017) Distinct global warming rates tied to multiple ocean surface temperature changes. Nat Clim Chang 7:486–491
Zhang C, Li S, Luo F, Huang Z (2019) The global warming hiatus has faded away: An analysis of 2014–2016 global surface air temperatures. Int J Climatol 39:4853–4868
IPCC, 2013: Climate Change 2013: The physical Science Basis. In: Contribution of Working Group I to the Fifth Assessment Report of the Intergovernmental Panel on Climate Change. Cambridge University Press, 1535 pp.
IPCC, 2021: Summary for policymakers. Climate Change 2021: The Physical Science Basis. In: V. Masson-Delmotte et al., Eds., Contribution of Working Group I to the Sixth Assessment Report of the Intergovernmental Panel on Climate Change; IPCC.

Publisher's Note